JOURNAL OF VIROLOGY, Dec. 2001, p. 12382–12392 Vol. 75, No. 24
0022-538X/01/$04.00+0 DOI: 10.1128/JVI.75.24.12382–12392.2001

Widespread Gene Delivery and Structure-Specific Patterns of Expression in the Brain after Intraventricular Injections of Neonatal Mice with an Adeno-Associated Virus Vector

MARCO A. PASSINI AND JOHN H. WOLFE*

Department of Pathobiology and Center for Comparative Medical Genetics, School of Veterinary Medicine, University of Pennsylvania, and Children's Hospital of Philadelphia, Philadelphia, Pennsylvania 19104

Received 6 July 2001/Accepted 11 September 2001

Developing a system for widespread somatic gene transfer in the central nervous system (CNS) would be beneficial for understanding the global influence of exogenous genes on animal models. We injected an adeno-associated virus serotype 2 (AAV2) vector into the cerebral lateral ventricles at birth and mapped its distribution and transduction pattern from a promoter capable of expression in multiple targets. The injections resulted in structure-specific patterns of expression that were maintained for at least 1 year in most regions, with efficient targeting of some of the major principal neuron layers. The patterns of transduction were explained by circulation of the viral vector in the subarachnoid space via CSF flow, followed by transduction of underlying structures, rather than by progenitor cell infection and subsequent migration. This study demonstrates that gene transfer throughout the CNS can be achieved without germ line transmission and establishes an experimental strategy for introducing genes to somatic cells in a highly predictable manner.

Widespread somatic gene delivery to the central nervous system (CNS) is of general interest for genetically modifying brain cells without the disadvantages of germ line transmission. Somatic gene delivery eliminates the potential lethality associated with expression during the formation and patterning period of the brain, and it restricts the genetic modifications only to cells of the CNS without involving other organ systems.

One strategy for widespread gene delivery is to inject viral vectors directly into the cerebral lateral ventricles and allow the natural flow of the cerebrospinal fluid (CSF) to deliver the virus throughout the CNS. However, when injected into the adult brain, adenovirus, adeno-associated virus serotype 4 (AAV4), or AAV5 vectors have not produced widespread transduction, due to their high affinity for the ependymal cells lining the ventricles (4, 13, 25, 34). Using a viral vector that is not absorbed and sequestered by the ependyma may allow the virus to gain access to a multitude of locations via the subarachnoid space. This has been tested with AAV2 in the adult brain, where the pia-arachnoid and hypothalamus became transduced, which suggests that these vectors are able to gain entry and circulate within the subarachnoid space (1, 41, 55). However, the extent of transduction was limited even with the aid of irradiation (1). The neonatal mouse brain may represent a window of opportunity for widespread gene transfer, since ongoing brain remodeling may help establish a substantial transduction profile along the CNS axis.

In this study, we injected an AAV2 vector into the cerebral lateral ventricles of mice at birth and used carbocyanine (CY3)-labeled virions and in situ hybridization as direct marker assays for vector distribution and expression, respectively. The data showed global delivery of AAV2 via the CSF and subsequent structure-specific patterns of gene expression that were sustained for at least 1 year in most structures. The principal neuron layers of the olfactory bulb, dentate gyrus, and cerebellar cortex were extensively transduced, demonstrating a potentially powerful strategy to target these specialized layers of major output neurons for genetic manipulation. The reproducibility of the transduction patterns shows that this experimental strategy can be used to deliver foreign genes throughout the CNS in a highly predictable manner.

* Corresponding author. Mailing address: 502 Abramson Research Center, Children's Hospital of Philadelphia, 3516 Civic Center Blvd., Philadelphia, PA 19104-4318. Phone: (215) 590-7028. Fax: (215) 590-3779. E-mail: jhwolfe@vet.upenn.edu.

MATERIALS AND METHODS

AAV2 genomic vector construction and packaging. The AAV2 genomic plasmid pTR-UF4 (a gift from N. Muzyczka) was modified as follows: the 1.8-kb NSE promoter was replaced with a 2.6-kb cassette (HβH) that contained the 0.4-kb human β-glucuronidase (GUSB) promoter immediately upstream of the 2.2-kb human GUSB cDNA (53). All bacterial transformations were performed in SURE-2 competent cells (Stratagene). Large-scale plasmid preps of the recombinant genome were performed (Maxiprep kit; Qiagen) and later packaged into AAV2 capsids by the Institute for Human Gene Therapy Vector Core using previously described methods (18). The virions generated were named AAV2-HβH and possessed a wild-type genome size of 4.7 kb and a titer of 4.5×10^{12} genome particles/ml, as determined by PCR of the simian virus 40 poly(A) sequence.

Experimental animals and intraventricular injection of AAV2-HβH. Normal C3H/HeOuJ mice were purchased from Jackson Laboratory (Bar Harbor, Maine) and maintained in our breeding colony. On the day of birth, designated as P0.5, pups were individually anesthetized on ice, and 2 μl of AAV2-HβH was injected into each lateral ventricle with a finely drawn glass micropipette needle (47). The viral solution contained 0.05% (wt/vol) trypan blue to help determine if the ventricles were indeed injected. Only those pups in which the lateral ventricles were filled with viral solution were analyzed; pups with misplaced parenchymal injections were not included in this study. All treatment of mice were approved by, and carried out according to the guidelines of, the Institutional Animal Care and Use Committee.

Preparation of brain. Mice to be sacrificed were deeply anesthetized and perfused transcardially with 1× PBS, which was followed by ice-cold fixative (4% paraformaldehyde–0.1 M phosphate buffer, pH, 7.4). Brains were dissected and refixed overnight at 4°C. Fixed tissues were cryoprotected overnight in 30% sucrose–0.1 M phosphate buffer at 4°C and placed in embedding medium, which consisted of 1 part 100% optimal cutting temperature (OCT) compound and 1 part 30% sucrose–0.1 M phosphate buffer. Tissues were frozen in liquid nitrogen-

cooled isopentane and stored at −80°C until ready for sectioning. Coronal serial sections were cut to a thickness of 20 μm and mounted on glass slides. Tissues designated for enzyme histochemistry were stored at −20°C, and those designated for in situ hybridization were stored at −80°C.

Enzyme histochemistry. Frozen tissue sections were assayed for enzymatic activity by staining with a naphthol-AS-BI-β-D-glucuronide substrate as reported (54). The very low levels of endogenous GUSB in the brain of C3H/HeOuJ mice is not detectable by this assay and can be used to study exogenous GUSB enzymatic activity. A further advantage of using the human GUSB cDNA is that the human protein is not heat labile, whereas the murine protein is inactivated at 65°C. To further ensure that GUSB-positive cells were from the vector, tissue sections were heat inactivated as reported (10).

In situ hybridization. To detect viral message, nonradioactive in situ hybridization was done on frozen tissue sections. Full-length human GUSB cDNA was cloned into Bluescript (Stratagene) and linearized to generate sense and antisense templates for runoff transcription from the cis-acting viral promoters. Antisense and sense digoxigenin-labeled (Roche) cRNA probes were generated and analyzed on a formaldehyde gel to verify probe length, and their ability to react with antidigoxigenin antibody was tested by using a dot blot assay. The in situ hybridization protocol was similar to that published elsewhere (39), with the following modifications: tissue sections were digested in proteinase K (10 μg/ml) for 5 min at 37°C, antisense or sense probes were mixed in hybridization solution at a concentration of 1 μg/ml and hybridized overnight at 60°C, and the antidigoxigenin antibody that is conjugated to alkaline phosphatase (Roche) was used at a dilution of 1:2,500. Sections from both enzyme histochemistry and in situ hybridization reactions were mounted in 100% glycerol and photographed by using Nomarski and light microscopy (Zeiss).

Fluorescent labeling of AAV2-HβH with CY3. The carbocyanine dye CY3 was covalently linked to the protein coat of AAV2-HβH virions according to the CyDye-FluoroLink labeling kit protocol (Amersham-Life Sciences) (5, 32). Unconjugated dye molecules were separated from labeled virions by dialyzing the reaction mixture in a dialysis chamber (molecular weight cutoff, 7,000; Slide-a-Lyser; Pierce) against three changes of 10 mM Tris-HCl (pH 7.5)–150 mM NaCl–10% glycerol at 4°C over a 24-h period. Purified CY3-labeled virions were brought up to 20% glycerol and stored at −80°C until ready for use. The CY3-labeled virions were injected into both lateral ventricles at P0.5, as described above. As a control for unlinked CY3 dye molecules, a separate tube containing saline was mixed with CY3, dialyzed, and injected into both lateral ventricles. Pups from the experimental and control injections were sacrificed either 30 min or 20 h later and fixed in toto for 48 h in 4% paraformaldehyde–0.1 M phosphate buffer, pH 7.4. The pups were then cryoprotected, frozen, sectioned, and stored at −20°C as described above. For analysis, sections were thawed, coverslips were mounted on the sections with a Vectashield-DAPI solution (Vector Laboratories), and the sections were photographed on a confocal microscope using Texas red and DAPI (4′,6′-diamidino-2-phenylindole) fluorescent filters.

RESULTS

The distribution of AAV2 virions after intraventricular injection. The distribution of AAV2 through the brain was determined with virions that were covalently labeled with CY3 fluorescent molecules (CY3-AAV2). CY3-AAV2 was injected into the cerebral lateral ventricles of newborn mice and analyzed 30 min and 20 h later. The resultant distribution patterns were similar at both time points; however, the rostral forebrain possessed more positive signals at 30 min compared to 20 h, whereas the caudal forebrain, midbrain, and hindbrain were more prominently labeled at 20 h. As a control for unlinked CY3 dye molecules, one litter received intraventricular injections of saline that went through the CY3 labeling protocol. These saline-injected neonates did not show fluorescent signals in any CNS structure, as illustrated by the rostral forebrain. (Fig. 1A).

Thirty minutes after the administration of CY3-AAV2, the rostral forebrain was symmetrically labeled along the ventral-dorsal axis of the midline and along the medial-lateral axis of the ventral surface (Fig. 1B and C). The strong labeling of cells was also present in more posterior structures, such as the hypothalamus and amygdala, in which a striking symmetry of fluorescent cells was observed in both hemispheres (Fig. 1D).

At twenty hours postinjection (p.i.), CY3-AAV2 was detected in many caudal brain structures. The neocortex was heavily labeled in both hemispheres, particularly along the surfaces in direct contact with the subarachnoid space, such as the quadrigeminal cistern (Fig. 1E). Labeling was also detected in the midbrain, as demonstrated by a high magnification image of the superior colliculus (Fig. 1F). In general, these high-magnification images showed fluorescent label in a punctate pattern which surrounded the DAPI-stained nuclei. These probably represent clusters of AAV2 virions accumulating in the perinuclear space, a feature of the normal AAV2 infection pathway (6). In more-ventral locations of the caudal brain, fluorescent label was detected along the surface of the parasubiculum and entorhinal cortex and lateral midbrain (Fig. 1G). High magnification of the entorhinal cortex showed fluorescence in cells adjacent to the ambient cistern of the subarachnoid space and within the neuropil (Fig. 1H). In the hindbrain, abundant fluorescence was detected along the ventral surface of the medulla (Fig. 1I). In addition, CY3-AAV2 was observed in the meninges and in the spaces between the lobules of the cerebellar cortex (Fig. 1J and K).

Of particular interest was the lack of fluorescent labeling in the subventricular germinal zone and along the lining of the cerebral lateral ventricle (Fig. 1L). This was consistent with the lack of AAV2 vector expression in the ependymal cell layers at all time points examined (data not shown).

The early AAV2 transduction pattern after intraventricular injection. The early transduction pattern of the AAV2-HβH vector, which contains the human GUSB promoter upstream of the human GUSB cDNA, was analyzed 1 week after intraventricular injections by in situ hybridization (Fig. 2). This time point was chosen to ensure that the rate-limiting second-strand synthesis step of the AAV2 vector was completed, thus allowing the viral vector to be fully capable of transcription (16, 17). Transferred gene expression was measured by comparing the AAV2-injected mice with control mice that were injected with saline. In all cases, no cells were in situ-hybridization positive in the brain of saline-injected mice. Furthermore, no cells were positive for the riboprobe after the injection of an AAV2 vector that contained a different cDNA directly into the brain parenchyma (data not shown). This additional control shows that the presence of AAV2 virions alone does not up-regulate endogenous mRNA levels.

The pattern of in situ-hybridization-positive cells at 1 week was similar to the distribution of CY3-AAV2 virions. Transduction was observed along the pial surface in contact with the subarachnoid space, within superficial layers of the brain parenchyma, and in the meninges (Fig. 2). This indicated that the AAV2 virions transduced the brain structures underlying the subarachnoid space following early circulation.

Most transduced brain structures sustained long-term viral vector expression. The expression pattern from the AAV2-HβH vector was analyzed at 1, 6, and 12 months p.i. ($n = 3$ for all groups). One month was chosen as a time point to investigate the postnatal transduction profile of the AAV2 vector, since organogenesis and the remodeling period of the CNS are completed by this time (47). The 6- and 12-month time points were analyzed to understand the effectiveness of the human

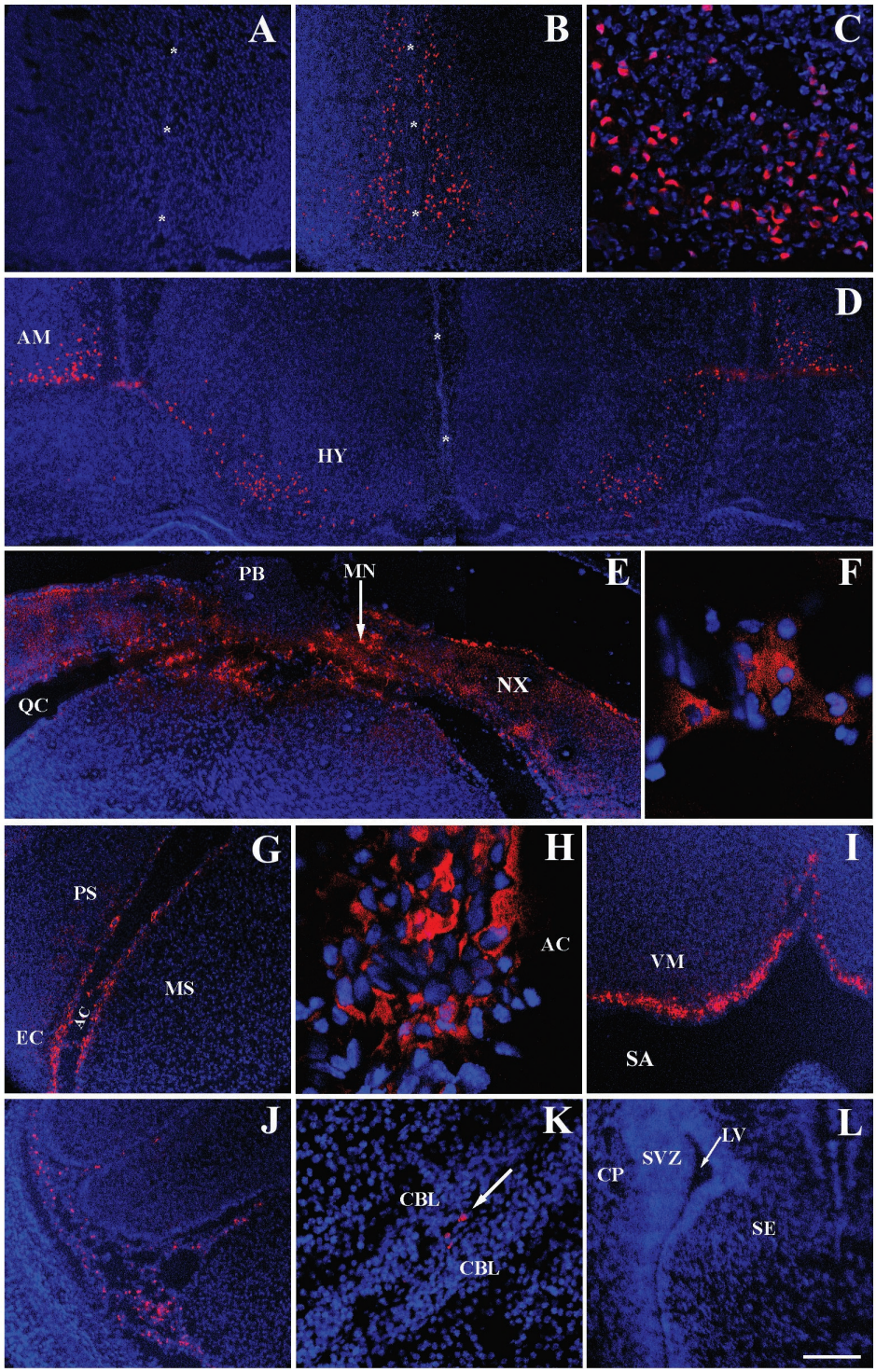

FIG. 1. CY3-AAV2 fluorescence after intraventricular injection at birth. The distribution of CY3-AAV2 virions was analyzed 30 min (A to D and L) and 20 h (E to K) after injection into the developing brain. Cells infected with CY3-AAV2 produced a red fluorescent color. Cell nuclei were visualized with the blue fluorochrome DAPI. Saline-injected mice produced no CY3 fluorescence (A). CY3-AAV2 was observed bilaterally along the midline (asterisks) of the rostral brain (B). (C) High magnification of panel B at the level of the ventral midline. Symmetrical infection was also observed in the amygdala and hypothalamus (D) and in the caudal brain (E). Abundant fluorescent signals were concentrated in the neocortex and meninges, whereas the pineal body, a gland in direct contact with the CSF, was negative for CY3-AAV2 (E). Magnification (×100) of the superior colliculus (F) and entorhinal cortex (H) demonstrated that the majority of CY3 signals were localized outside the nucleus. CY3 fluorescence was detected along the lining of the ambient cistern (G). CY3-AAV2 was abundant along the surface of the ventral medulla (I) and circulating in spaces between the lobules of the cerebellar cortex (J and K [arrow]). Fluorescence was observed neither in the cerebral lateral ventricle nor in the subventricular zone and adjacent brain structures (L). Scale bars: 200 μm (A, B, D, E, G, I, J, and L), 50 μm (C and K), and 20 μm (F and H). Abbreviations: AC, ambient cistern; AM, amygdala; CBL, cerebellar lobules; CP, caudate putamen; EC, entorhinal cortex; HY, hypothalamus; LV, cerebral lateral ventricle; MN, meninges; MS, lateral midbrain; NX, neocortex; PB, pineal body; PS, parasubiculum; QC, quadrigeminal cistern; SA, subarachnoid space; SE, septum; SVZ, subventricular zone.

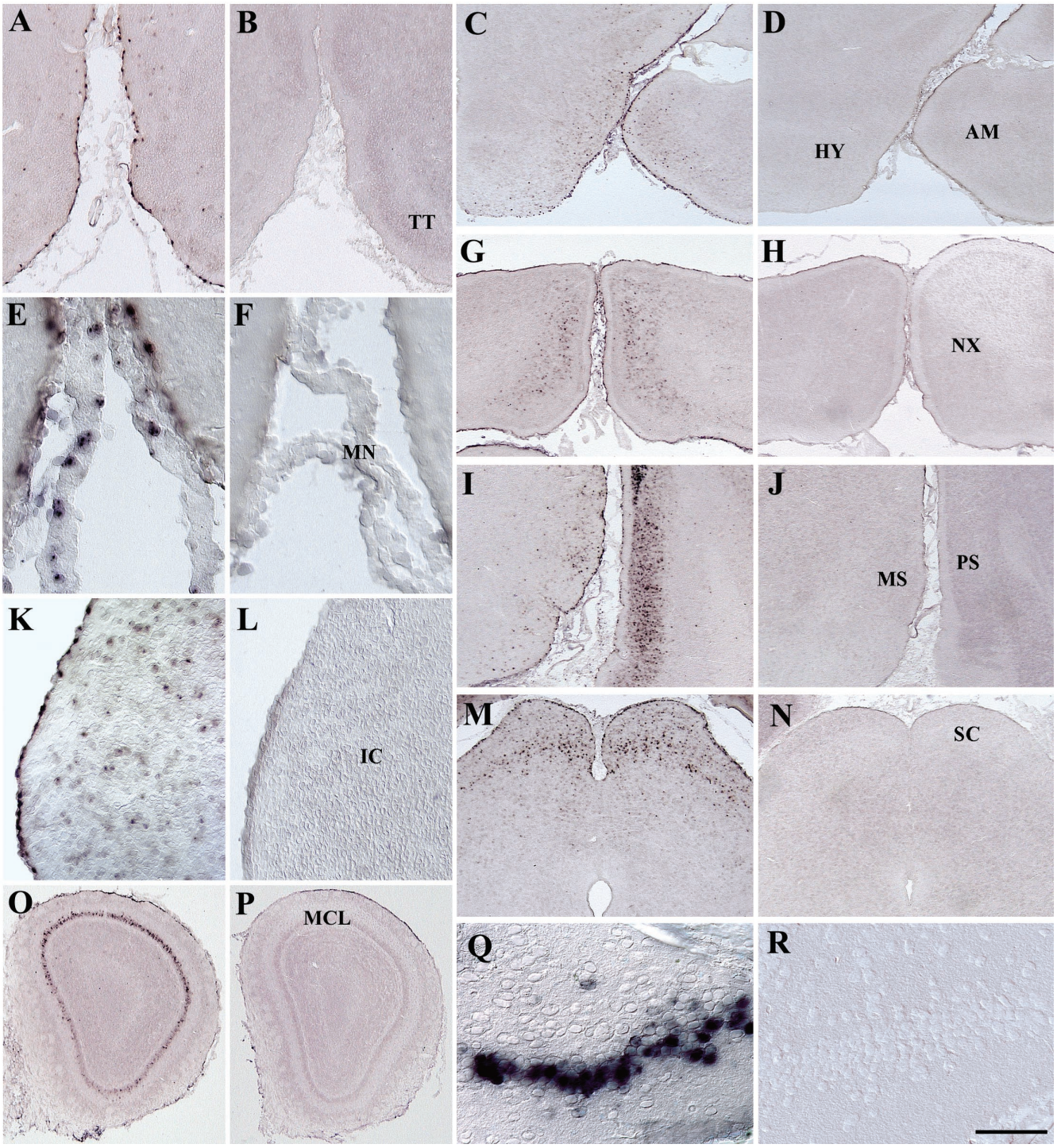

FIG. 2. Analysis of the transduction pattern 1 week after intraventricular injection of P0.5 mice. AAV2-HβH transduction was observed in the pial surface, brain parenchyma, and meninges of vector-injected (A, C, E, G, I, K, M, O, and Q) but not saline-injected (B, D, F, H, J, L, N, P, and R) control brains. Robust expression was also detected in the MCL of the main olfactory bulb (O) and in the ventralmost region of the granule cell layer of the dentate gyrus (Q). This ventralmost region is in direct contact with the CSF via the interpeduncular cistern and may provide an accessible pathway for AAV2 penetration into the dentate gyrus. Scale bars: 200 μm (A and B), 500 μm(C, D, G, H, I, J, M, N, O, and P), 60 μm (E, F, Q, and R), and 100 μm (K and L). Abbreviations: IC, inferior colliculus; SC, superior colliculus; TT, tenia tecta. See Fig. 1 legend for other abbreviations.

GUSB promoter to maintain long-term expression. Previous reports with adult rodent brain injections have demonstrated that the site and duration of AAV2 vector expression varied in different structures (28, 38). The human GUSB promoter was therefore used in this study since this regulatory element achieved high levels of expression in all tissues of transgenic mice and in ex vivo gene transfer experiments in the adult mouse brain (31, 50).

TABLE 1. Summary of distinct and reproducible patterns of transduction in structures of the CNS following intraventricular injection of AAV2-HβH

Pattern	Structure	Expression[a] at mo:		
		1	6	12
High initial transduction, sustained expression	Amygdala	+++	+++	++
	Dorsal and ventral horns, SC	++	++	++
	Hypothalamus	+++	+++	++
	Inferior colliculus	++++	+++	+++
	Medulla oblongata	+++	+++	+++
	Mitral cell layer, OB	++++	++++	+++
	Olfactory tubercle	+++	+++	++
	Parasubiculum	+++	+++	+++
	Purkinje cell layer, CB	+++	+++	++
	Subiculum	++	++	++
	Superior colliculus	+++	+++	+++
Low initial transduction, sustained expression	CA1/CA3 pyramidal layers, HP	+	+	+
	Caudate putamen	±	−	−
	Geniculate	±	±	±
	Inner tier, granule cell layer, DG	±	±	−
	Interneuron layers, OB	+	±	±
	Septum	±	−	−
	Substantia nigra	±	±	−
High initial transduction, decreased expression	Neocortex	+++	+	+
	Outer tier, granule cell layer, DG	++++	+++	+

[a] Expression based on the number of in situ-hybridization-positive cells in one hemisphere. Symbols: ++++, 201 cells or more; +++, 101 to 200 cells; ++, 31 to 100 cells; +, 10 to 30 cells; ±, 1 to 9 cells; −, no cells. Abbreviations: CB, cerebellum; DG, dentate gyrus; HP, hippocampus; OB, olfactory bulb; SC, spinal cord.

Intraventricular injections at birth resulted in structure-specific patterns of gene expression that were highly reproducible in all infected mice. The expression patterns were based on how the relative number of in situ-hybridization-positive cells changed with time within a given structure (Table 1). All patterns were similar in both hemispheres, as demonstrated by multiple brain structures at the level of the caudal forebrain/rostral midbrain (Fig. 3A and B). In situ hybridization using sense riboprobes was done as a negative control on all brain sections and produced little or no positive signal (Fig. 3C).

Enzyme histochemical reactions showed that functional GUSB protein was translated from the viral message (Fig. 3B). The normal C3H mouse contains very low levels of GUSB activity in the brain, which can be heat inactivated relative to the human protein (10, 26, 40). Uninjected C3H mice were always negative for enzyme histochemistry in all brain structures (Fig. 3D), confirming that the enzymatic activity seen was not due to endogenous GUSB.

The most-common pattern showed high numbers of transduced cells within a given structure, and these numbers were sustained for at least 1 year p.i. (Table 1). A typical example of this transduction pattern is illustrated by the inferior colliculus. Numerous in situ-hybridization and enzyme-positive cells were evenly distributed in both hemispheres at 1 month p.i. (Fig. 3E and F). Although there was a small decrease in the number of positive cells with time, a substantial number of cells remained positive at 6 (Fig. 3G and H) and 12 months (Fig. 3I and J).

A group of brain structures showed low transduction, which did not increase with time (Table 1). All brain structures that possessed low transduction, such as the caudate putamen and septum, contained very little CY3 fluorescence shortly after injection, indicating that AAV2 did not gain access to these structures via the CSF. This was also supported by results of direct injections of AAV2-HβH into these structures in the adult mouse brain, where high levels of expression occurred (data not shown).

Expression in the neocortex and hippocampus decrease with time. A distinct pattern of expression was observed in the neocortex and in the dentate gyrus of the hippocampal formation. In both structures, high numbers of in situ-hybridization-positive cells were detected at 1 month but were not sustained over time (Table 1).

In the neocortex, the temporal pattern of expression involved the transduction of cells at 1 month p.i. (Fig. 4A), followed by a substantial decrease in the number of in situ-hybridization-positive cells at 6 months (Fig. 4B), which then remained constant at 12 months (Fig. 4C). At all time points, positive cells were found scattered in all layers of the neocortex, with the most-numerous cells being detected in layers II to V. In general, transduced cells were more numerous in the neocortex of the caudal forebrain compared to that of the rostral forebrain. This corresponds to the distribution of the viral vector after injection, in which CY3-fluorescent signals were present in greater concentration in the caudal areas of the neocortex.

In the hippocampus, abundant cells were positive for AAV2 vector expression in the granule cell layer (GCL) of the dentate gyrus at 1 month p.i. (Fig. 4D and E). However, transduction was restricted to the outer tier of the GCL, on the side directly adjacent to the molecular layer. A decline in the number of positive cells was apparent by 6 months (Fig. 4F and G), which further decreased at 12 months (Fig. 4H and I).

Transduction of principal neuron layers. Extensive transduction occurred in the principal neuron layers of the dentate gyrus, olfactory bulb, and cerebellar cortex. Principal neurons, also known as relay or projection neurons, receive synaptic input from multiple sources and then convey that information

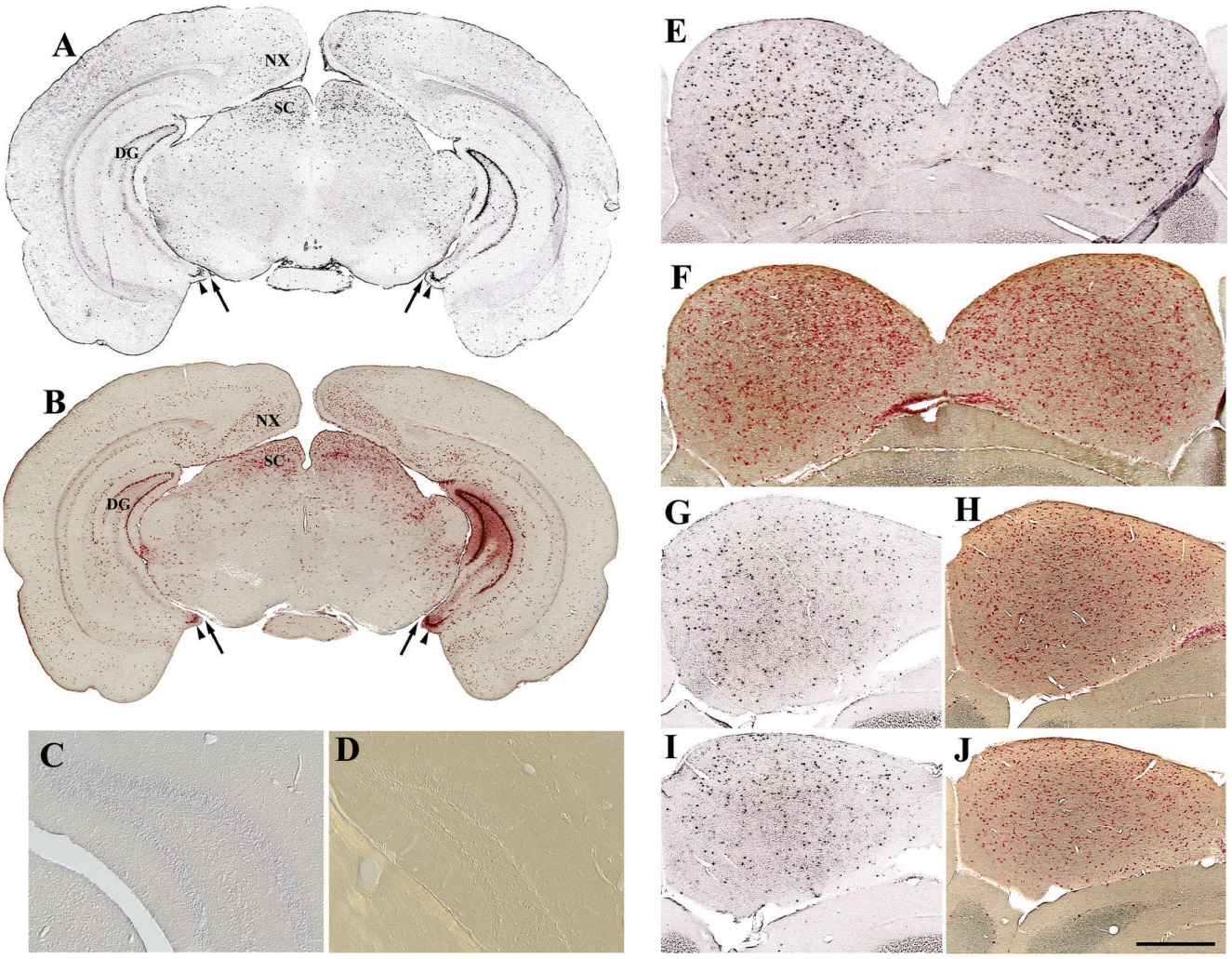

FIG. 3. Symmetrical and sustained expression from AAV2-HβH following intraventricular injections at birth as shown by in situ hybridization (A, C, E, G, and I) and enzyme histochemistry (B, F, H, and J). Symmetrical pattern of positive cells at the level of the caudal forebrain-rostral midbrain at 1 month p.i. (A and B). The relative positions between the interpeduncular cistern (arrow) and ventral dentate gyrus (arrowhead) are shown. The dentate gyrus of injected brain was negative with a sense riboprobe (C). The dentate gyrus of normal, uninjected C3H mice does not produce detectable levels of enzyme activity (D). (E to J) AAV2 vector expression in the inferior colliculus. Numerous cells were positive for human GUSB at 1 (E and F), 6 (G and H), and 12 (I and J) months p.i. Scale bars: 1.25 mm (A and B), 250 μm (C and D), and 500 μm (E to J). Abbreviations: DG, dentate gyrus; SC, superior colliculus. See Fig. 1 legend for other abbreviations.

to other brain centers through interregional pathways that typically involve long axon projections (45). The principal neurons of the dentate gyrus, olfactory bulb, and cerebellar cortex are present in specific layers that are distinct and separate from the surrounding interneuronal and plexiform layers.

In the dentate gyrus, the principal neurons are granule cells, which send axons to CA3 pyramidal cells of the hippocampus. At birth, the outer tier of the GCL contains a population of mature granule cells, whereas the inner tier is composed of immature granule cells and dividing progenitors (11, 14, 42). The restriction of gene expression to the outer but not the inner tier indicated that selective targeting of principal neurons occurred after vector administration (Fig. 4E, G, and I). If dividing progenitor cells had been transduced at birth, AAV2 vector expression would be expected to be detected in the inner tier of the GCL due to the ongoing addition of granule cells that occurs in the adult rodent (2, 7, 20, 43).

In the olfactory bulb, the principal neurons are mitral cells, which send long axonal projections via the lateral olfactory tract to the paleocortex. An extensive pattern of transduction was observed in the mitral cell layer (MCL) at all time points examined (Fig. 5A to E). High magnification of the MCL showed that the positive label was restricted primarily to large cell bodies, which contained dendrites that extended into the external plexiform layer, a hallmark feature of mitral cell morphology (45) (Fig. 5D). Nearly all of the large cell bodies in this layer were positive by in situ hybridization, while the small, unlabeled cell bodies adjacent to the inner plexiform layer were displaced granule interneurons (8) (Fig. 5E). Analysis of a 6-month-old transgenic adult mouse, which expresses the human GUSB gene from the human GUSB promoter on a null background (31), showed in situ-hybridization-positive signals in all cell layers of the olfactory bulb (Fig. 5F). This demonstrated that the human GUSB promoter is capable of expres-

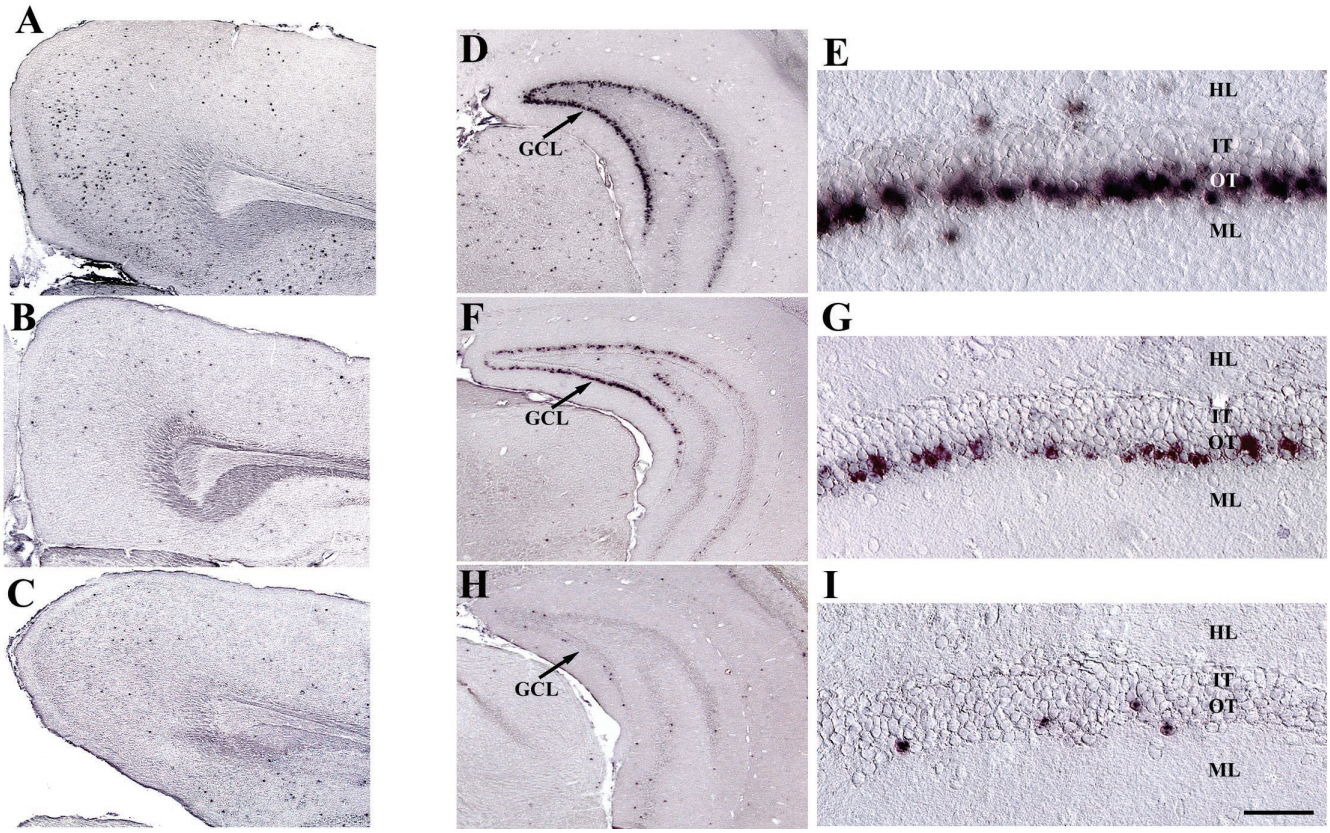

FIG. 4. Decreased expression with time in the neocortex and dentate gyrus. Shown is AAV2-HβH expression in the neocortex (A to C) and dentate gyrus (D to I). The number of in situ-hybridization-positive cells in the neocortex at 1 month (A) was substantially greater than that at 6 (B) and 12 (C) months p.i. Abundant expression was detected in the GCL at 1 month p.i. (D and E), followed by a continual decrease in expression at 6 (F and G) and 12 (H and I) months p.i. Viral vector expression was confined to the outer tier of the GCL in all time points. Scale bars: 500 μm (A to D, F, and H) and 50 μm (E, G, and I). Abbreviations: HL, hilus; IT, inner tier of the GCL; ML, molecular layer of the dentate gyrus; OT, outer tier of the GCL.

sion in all cell layers, indicating that the AAV2 vector specifically transduced mitral cells.

In the cortex of the cerebellum, the principal neurons are Purkinje cells, which send axons to the deep cerebellar nuclei. In situ-hybridization-positive signals were present in the Purkinje cell layer of all lobules, with the most-numerous positive cells being located in the lobule directly adjacent to the fourth ventricle (Fig. 5G). High magnification images showed that nearly all of the positive signals were located in a single row of cells that extended dendrites into the molecular layer (Fig. 5H). The morphology and position within in the lobules clearly demonstrated that these were Purkinje cells.

Transduction of other principal neurons, identified by the morphology of their somas, also occurred. Neocortical pyramidal cells (Fig. 5I) and spinal cord motoneurons in the ventral horn (Fig. 5J) were consistently positive for in situ hybridization and enzymatic activity.

DISCUSSION

The AAV2 transduction patterns we observed after intraventricular injection of neonates, when the brain is undergoing significant remodeling, were unexpectedly widespread and have important implications for neuroscience and gene therapy experiments. Understanding the properties of AAV2 with this experimental strategy is critical to using them effectively as somatic gene transfer tools. This will be of general interest to those who want to achieve widespread genetic modification of cells without the disadvantages associated with transgenic animals.

A desirable feature of AAV vectors is that all the viral coding sequences are removed when engineering the recombinant genome, thereby limiting the extent of the cell toxicity and immune response that are often associated with viral gene expression (56). The efficient transduction of postmitotic cells by AAV make it an excellent vector to deliver genes to the CNS. In parenchymal injections, AAV2 vectors remain relatively confined to the injection site and show a substantial preference for transducing neurons over glia, which are due to the high abundance of heparan sulfate proteoglycans found on neuronal surfaces (5, 24, 37, 46). AAV2 binds heparan sulfate proteoglycans with high affinity and utilizes these molecules as a primary attachment receptor in cells (6, 49).

Although confinement of AAV2 vectors to the injection site is beneficial for localized gene delivery, widespread distribution of the viral vector would be desirable in experiments aimed at understanding the global influence of transferred genes on experimental and disease models. One potential

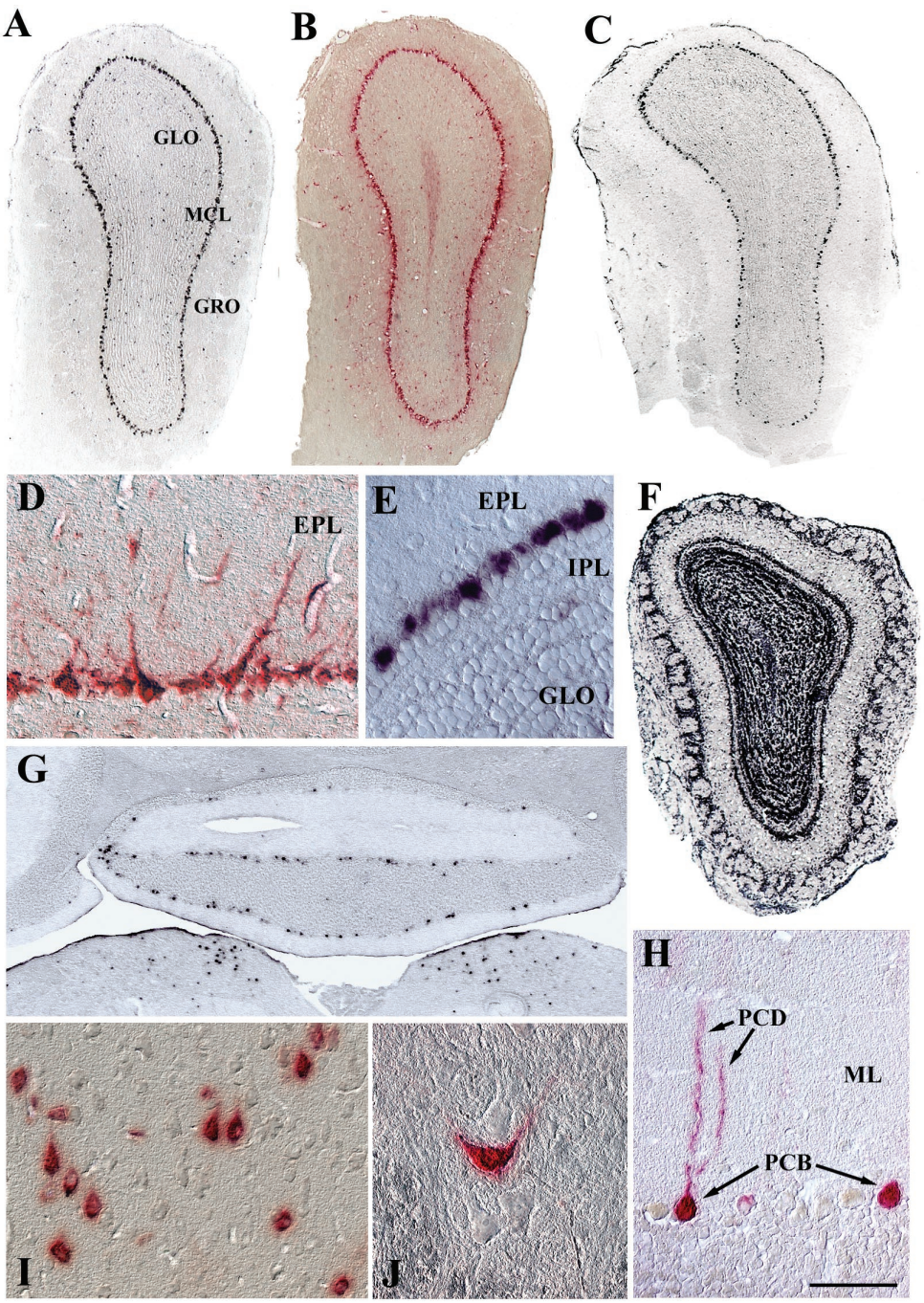

FIG. 5. Transduction of principal neuron layers as shown by in situ hybridization (A, C, E, F, and G) and enzyme histochemistry (B, D, and H to J). AAV2-HβH expression was detected throughout the MCL at 1 (A and B) and 12 (C, D, and E) months p.i. In addition, a small number of positive cells were scattered in the granule and glomerular layers (A to C). (F) An uninjected transgenic mouse showed that expression of the human GUSB promoter was not restricted to mitral cells. (G) Expression in the medulla oblongata (lower part of panel) and Purkinje cell layer of the cerebellar cortex at 1 month p.i. (H) Purkinje cell morphology was evident with enzyme histochemistry at 12 months p.i. (I) In the motor cortex at 6 months p.i., many enzyme-positive cells possessed pear-shaped somas, characteristic of pyramidal cell morphology. (J) The ventral horn at 12 months p.i. showed an enzyme-labeled neuron in a field of unlabeled neurons. Scale bars: 500 μm (A to C, F, and G) and 50 μm (D, E, and H to J). Abbreviations: EPL, external plexiform layer; GLO, olfactory granule cell layer; GRO, olfactory glomerular cell layer; IPL, inner plexiform layer; ML, molecular layer of the cerebellum; PCB, Purkinje cell bodies; PCD, Purkinje cell dendrites.

strategy for widespread gene delivery is to inject AAV2 directly into the cerebral lateral ventricles and allow the CSF stream to deliver the viral vector throughout the CNS. However, intraventricular injections into the adult brain with AAV2 results in limited CNS transduction in rodents (1, 13, 41, 55). The majority of transduced cells are restricted to CNS epithelial structures, particularly to the pia-arachnoid and leptomeninges (1, 41). PCR analysis for the AAV2 vector genome has shown that

the hypothalamus is transduced following adult intraventricular injection, but the medulla oblongata, neocortex, and cerebellum are not (55). This differs considerably from our study, in which all of these structures and many others are extensively transduced, indicating that penetration of AAV2 vectors into the brain parenchyma is a substantially more efficient process in the neonate compared to the adult.

One mechanism by which viral vectors have been shown to gain access to multiple structures in the developing brain is by infecting progenitor cells of the subventricular germinal zones, followed by expansion and subsequent migration of transduced cells through the brain parenchyma. Intraventricular injections with retroviruses in the developing brain resulted in neocortical expression that was generated and mediated by a progenitor cell infection step (51, 52). Furthermore, transplantation of engineered neural progenitor cells results in engraftment of germinal zones and migration of donor-derived cells in the CNS (29, 33, 47).

Our data demonstrate that distribution of AAV2 differs from retroviruses and neural cell transplants. When administered at birth, AAV2 does not undergo substantial diffusion into the subventricular germinal zones, but rather circulates through the subarachnoid space. This is supported by at least two lines of evidence. Firstly, CY3 fluorescence and the 1 week in situ hybridization, which showed the early p.i. distribution and transduction patterns, were not detected in subventricular germinal zones. Instead, positive cells were observed in the meninges, along the pial surface directly contacting the subarachnoid space, and within superficial locations of the brain parenchyma. Secondly, the transduction pattern observed in the MCL of the olfactory bulb is not consistent with delivery by the rostral migratory stream. If diffusion and subsequent transduction of progenitor cells in the anterior subventricular zone had occurred, it would be expected to result in vector expression being present in granule and periglomerular neurons, two cell types born postnatally (3, 36). Previous work demonstrated that adenovirus and retrovirus vectors are localized predominately to these two classes of interneurons following anterior subventricular zone injections in adult and neonatal rodents (36, 57). Neural progenitor cell transplantation studies have also shown that exogenous cells migrate down the rostral migratory stream and differentiate into granule and periglomerular cells, but not into mitral cells (35).

Of particular interest is the extent of transduction that occurred in the mitral cells of the olfactory bulb. The lack of CY3 fluorescence along the pial surface and olfactory ventricle of the main olfactory bulb suggests that the AAV2 vector did not gain access to the mitral cell bodies by the CSF. One potential explanation is that the AAV2 transduced mitral cells at distant locations and moved by retrograde transport through the lateral olfactory tract. All mitral cells are born by embryonic day 17 in rodents and send projections to the paleocortex, a region of the ventral forebrain that includes the olfactory tubercle, piriform and entorhinal cortexes, and amygdala (8, 23, 45). Abundant CY3-AAV2 virions and in situ-hybridization-positive cells were detected in the paleocortex. A mechanism of infection at the distal end of the nerve, followed by retrograde transport to mitral cell bodies would explain the observed expression pattern in the olfactory bulb. Although retrograde transport does not appear to be a general property of AAV2 vectors, a recent report showed that axonal transport occurs in the Purkinje cells of the cerebellum after injection of the viral vector into the deep cerebellar nuclei of adult mice (27). Since Purkinje cells are a type of principal neuron, that experiment taken with our data suggest that axonal transport of AAV2 vectors may be a property of principal neurons.

In the majority of transduced structures, expression at 1 month p.i. was maintained at 6 and 12 months, demonstrating the effectiveness of the human GUSB promoter to support long-term expression in a wide variety of CNS structures. However, two structures showed a substantial decrease in the number of in situ-hybridization-positive cells over time. The gradual loss of positive cells in the dentate gyrus is consistent with the progressive cell turnover that occurs in the GCL throughout the life span of the adult rodent (7, 22). In contrast, the decline of vector gene expression in the neocortex between 1 and 6 months may be due to suppression of promoter activity rather than cell loss, since developmental pruning of neurons in the neocortex is completed by 1 month.

In some inherited neurodegenerative diseases, notably the lysosomal storage disorders, it is possible to treat the brain by transducing a limited number of cells and relying on export of the therapeutic protein for uptake by cells in distal structures. This has been clearly demonstrated by a number of laboratories using GUSB in the mucopolysaccharidosis type VII mouse brain (9, 12, 15, 19, 21, 30, 44, 46–48, 50). The widespread distribution of GUSB activity seen in the present study is well above the amount previously proven to be therapeutic for the mucopolysaccharidosis type VII mouse brain. For other inherited diseases that affect the entire CNS, it will be important to deliver the gene itself to a global population of cells, since most neurodegenerative diseases do not involve secretory proteins. Although our experiments show that a gene can be transferred widely in the brain, not all neurons were transduced, which may limit the therapeutic efficacy for some disorders.

Future studies should be conducted to understand the postpartum time frame in which AAV2 is able generate this extensive transduction pattern. Defining the temporal window of opportunity for widespread gene delivery, before the brain adopts the more limited adult pattern, would be relevant for designing both functional and treatment strategies.

Introducing viral vectors into the cerebral lateral ventricles at birth is a relatively easy and effective alternative to multiple parenchymal injections for achieving widespread gene delivery. The global targeting and transduction of the CNS reported in this study resulted in very robust expression compared to previous adult and neonatal intraventricular injections, in which transduction with a variety of viral vectors was limited (1, 13, 51, 52, 55). The human GUSB promoter demonstrated the ability of the AAV2 vector to function in multiple brain structures. It may also be possible to express foreign genes in specific target structures by using cell type-specific promoters. The reproducibility of the structure-specific patterns of gene expression and efficient transduction of principal neuron layers allow this experimental strategy to be used in a predictable manner. The defined strategy of genetic modifications of somatic cells reported in this study should have wide applicability for manipulations in the CNS.

ACKNOWLEDGMENTS

We thank G. Heuer for his assistance with the neonatal injections, A. Polesky for her help with the cryosectioning, S. Puhalla for help with confocol imaging, and G. Gao and G. Qu for their help with viral production.

This work was supported by NIH grants DK46637 and NS38690 to J.H.W. and by the Gene Therapy Core Center (DK47747), and M.A.P. was supported by NRSA training grant DK07748.

REFERENCES

1. **Alexander, I. E., D. W. Russell, A. M. Spence, and A. D. Miller.** 1996. Effects of gamma irradiation on the transduction of dividing and nondividing cells in brain and muscle of rats by adeno-associated virus vectors. Hum. Gene Ther. **7:**841–850.
2. **Altman, J., and G. D. Das.** 1965. Autoradiographic and histological evidence of postnatal hippocampal neurogenesis in rats. J. Comp. Neurol. **124:**319–335.
3. **Altman J.** 1969. Autoradiographic and histological studies of postnatal neurogenesis. IV. Cell proliferation and migration in the anterior forebrain, with special reference to persisting neurogenesis in the olfactory bulb. J. Comp. Neurol. **137:**433–457.
4. **Bajocchi, G., S. H. Feldmann, R. G. Crystal, and A. Mastrangeli.** 1993. Direct *in vivo* gene transfer to ependymal cells in the central nervous system using recombinant adenovirus vectors. Nat. Genet. **3:**229–234.
5. **Bartlett, J. S., R. J. Samulski, and T. J. McCown.** 1998. Selective and rapid uptake of adeno-associated virus type 2 in brain. Hum. Gene Ther. **9:**1181–1186.
6. **Bartlett, J. S., R. Wilcher, and R. J. Samulski.** 2000. Infectious entry pathway of adeno-associated virus and adeno-associated virus vectors. J. Virol. **74:**2777–2785.
7. **Bayer, S. A.** 1982. Changes in the total number of dentate granule cells in juvenile and adult rats: a correlation volumetric and ^{3}H-thymidine autoradiographic study. Exp. Brain Res. **46:**315–323.
8. **Bayer, S. A.** 1983. ^{3}H-thymidine-radiographic studies of neurogenesis in the rat olfactory bulb. Exp. Brain Res. **50:**329–340.
9. **Bosch, A., E. Perret, N. Desmaris, D. Trono, and J. M. Heard.** 2000. Reversal of pathology in the entire brain of mucopolysaccharidosis type VII mice after lentiviral-mediated gene transfer. Hum. Gene Ther. **11:**1139–1150.
10. **Casal, M. L., and J. H. Wolfe.** 2001. *In utero* transplantation of fetal liver cells in the mucopolysaccharidosis type VII mouse results in low-level chimerism, but overexpression of β-glucuronidase can delay onset of clinical signs. Blood **97:**1625–1634.
11. **Crespo, D., B. B. Stanfield, and W. M. Cowan.** 1986. Evidence that late-generated granule cells do not simply replace earlier formed neurons in the rate dentate gyrus. Exp. Brain Res. **62:**541–548.
12. **Daly, T. M., C. Vogler, B. Levy, M. E. Haskins, and M. S. Sands.** 1999. Neonatal gene transfer leads to widespread correction of pathology in a murine model of lysosomal storage disease. Proc. Natl. Acad. Sci. USA **96:**2296–2300.
13. **Davidson, B. L., C. S. Stein, J. A. Heth, I. Martins, R. M. Kotin, T. A. Derksen, J. Zabner, A. Ghodsi, and J. A. Chiorini.** 2000. Recombinant adeno-associated virus type 2, 4, and 5 vectors: transduction of variant cell types and regions in the mammalian central nervous system. Proc. Natl. Acad. Sci. USA **97:**3428–3432.
14. **Dupuy, S. T., and C. R. Houser.** 1997. Developmental changes in GABA neurons of the rat dentate gyrus: an *in situ* hybridization and birthdating study. J. Comp. Neurol. **389:**402–418.
15. **Elliger, S., C. Elliger, C. Aguilar, N. Raju, and G. Watson.** 1999. Elimination of lysosomal storage in brains of MPS VII mice treated with intrathecal administration of an adeno-associated virus vector. Gene Ther. **6:**1175–1178.
16. **Ferrari, F. K., T. Samulski, Y. Shenk, and R. J. Samulski.** 1996. Second-strand synthesis is a rate-limiting step for efficient transduction by recombinant adeno-associated virus vectors. J. Virol. **70:**3227–3234.
17. **Fisher, K. J., G. P. Gao, M. D. Weitzman, R. DeMatteo, J. F. Burda, and J. M. Wilson.** 1996. Transduction with recombinant adeno-associated virus for gene therapy is limited by leading-strand synthesis. J. Virol. **70:**520–532.
18. **Fisher, K. J., K. Jooss, J. Alston, Y. Yang, S. E. Haecker, K. High, R. Pathak, S. E. Raper, and J. M. Wilson.** 1997. Recombinant adeno-associated virus for muscle-directed gene therapy. Nat. Med. **3:**306–312.
19. **Frisella, W. A., L. H. O'Connor, C. A. Vogler, M. Roberts, S. Walkley, B. Levy, T. M. Daly, and M. S. Sands.** 2001. Intracranial injection of recombinant adeno-associated virus improves cognitive function in a murine model of mucopolysaccharidosis type VII. Mol. Ther. **3:**351–358.
20. **Gage, F. H.** 2000. Mammalian neural stem cells. Science **287:**1433–1438.
21. **Ghodsi, A., C. Stein, C., T. Derksen, I. Martins, R. D. Anderson, and B. L. Davidson.** 1999. Systemic hyperosmolality improves β-glucuronidase distribution and pathology in murine MPS VII brain following intraventricular gene transfer. Exp. Neurol. **160:**109–116.
22. **Gould, E., and H. A. Cameron.** 1996. Regulation of neuronal birth, migration, and death in the rat dentate gyrus. Dev. Neurosci. **18:**22–35.
23. **Hinds, J. W.** 1968. Autoradiographic study of histogenesis in the mouse olfactory bulb. I. Time of origin of neurons and neuroglia. J. Comp. Neurol. **134:**287–304.
24. **Hsueh, Y. P., F. C. Yang, V. Kharazia, S. Naisbitt, A. R. Cohen, R. J. Weinberg, and M. Sheng.** 1998. Direct interaction of CASK/LIN-2 and syndecan heparan sulfate proteoglycan and their overlapping distribution in neuronal synapses. J. Cell Biol. **142:**139–151.
25. **Johansson, C. B., S. Momma, D. L. Clarke, M. Risling, U. Lendahl, and J. Frisen.** 1999. Identification of a neural stem cell in the adult mammalian central nervous system. Cell **96:**25–34.
26. **Johnson, W. G., J. L. Hong, and S. M. Knights.** 1896. Variations in ten lysosomal hydrolase enzyme activities in inbred mouse strains. Biochem. Genet. **24:**891–909.
27. **Kaemmerer, W. F., R. G. Reddy, C. A. Warlick, S. D. Hartung, R. S. McIvor, and W. C. Low.** 2000. *In vivo* transduction of cerebellar Purkinje cells using adeno-associated virus vectors. Mol. Ther. **2:**446–457.
28. **Klein, R. L., E. M. Meyer, A. L. Peel, S. Zolotukhin, C. Meyers, N. Muzyczka, and M. A. King.** 1998. Neuron-specific transduction in the rat septohippocampal or nigrostriatal pathway by recombinant adeno-associated virus vector. Exp. Neurol. **150:**183–194.
29. **Kopen, G. C., D. J. Prockop, and D. G. Phinney.** 1999. Marrow stromal cells migrate throughout forebrain and cerebellum, and they differentiate into astrocytes after injection into neonate mouse brains. Proc. Natl. Acad. Sci. USA **96:**10711–10716.
30. **Kosuga, M., K. Sasaki, A. Tanabe, X. K. Li, H. Okawa, I. Ogino, O. Okuda, H. Arai, N. Sakuragawa, Y. Kamata, N. Azuma, S. Suzuki, M. Yamada, and T. Okuyama.** 2001. Engraftment of genetically engineered amniotic epithelial cells corrects lysosomal storage in multiple areas of the brain in mucopolysaccharidosis type VII mice. Mol. Ther. **3:**139–148.
31. **Kyle, J. W., E. H. Birkenmeier, B. Gwynn, C. Vogler, P. C. Hoppe, J. W. Hoffmann, and W. S. Sly.** 1990. Correction of murine mucopolysaccharidosis VII by a human β-glucuronidase transgene. Proc. Natl. Acad. Sci. USA **81:**6466–6470.
32. **Leopold, P. L., B. Ferris, I. Grinberg, S. Worgall, N. R. Hackett, and R. G. Crystal.** 1998. Fluorescent virions: dynamic tracking of the pathway of adenoviral gene transfer vectors in living cells. Hum. Gene Ther. **9:**367–378.
33. **Lim, D. A., G. J. Fishell, and A. Alvarez-Buylla.** 1997. Postnatal mouse subventricular zone neuronal precursors can migrate and differentiate within multiple levels of the developing neuroaxis. Proc. Natl. Acad. Sci. USA **94:**14832–14836.
34. **Lo, W. D., G. Qu, T. J. Sferra, R. Clark, R. Chen, and P. R. Johnson.** 1999. Adeno-associated virus-mediated gene transfer to the brain: duration and modulation of expression. Hum. Gene Ther. **10:**201–213.
35. **Lois, C., and A. Alvarez-Buylla.** 1994. Long-distance neuronal migration in the adult mammalian brain. Science **264:**1145–1148.
36. **Luskin, M. B.** 1993. Restricted proliferation and migration of postnatally generated neurons derived from the forebrain subventricular zone. Neuron **11:**173–189.
37. **Mandel, R. J., K. G. Rendahl, S. K. Spratt, R. O. Snyder, L. K. Cohen, and S. E. Leff.** 1998. Characterization of intrastriatal recombinant adeno-associated virus-mediated gene transfer of human tyrosine hydroxylase and human GTP-cyclohydrolase I in a rat model of Parkinson's disease. J. Neurosci. **18:**4271–4284.
38. **McCown, T. J., X. Xiao, J. Li, G. R. Breese, and R. J. Samulski.** 1996. Differential and persistent expression patterns of CNS gene transfer by an adeno-associated virus (AAV) vector. Brain Res. **713:**99–107.
39. **Passini, M. A., E. M. Levine, A. K. Canger, P. A. Raymond, and N. Schechter.** 1997. Vsx-1 and Vsx-2: differential expression of two paired-like homeobox genes during zebrafish and goldfish retinogenesis. J. Comp. Neurol. **388:**495–505.
40. **Pfister, K., K. Paigen, G. Watson, and V. Chapman.** 1982. Expression of β-glucuronidase haplotypes in prototype and congenic mouse strain. Biochem. Genet. **20:**519–536.
41. **Rosenfeld, M. R., I. Bergman, L. Schramm, J. A. Griffin, M. G. Kaplitt, and P. I. Meneses.** 1997. Adeno-associated viral vector transfer into leptomeningeal xenografts. J. Neurooncol. **34:**139–144.
42. **Schlessinger, A. R., W. M. Cowan, and D. I. Gottlieb.** 1975. An autoradiographic study of the time of origin and pattern of granule cell migration in the dentate gyrus of rat. J. Comp. Neurol. **159:**149–176.
43. **Seki, T., and Y. Arai.** 1993. Highly polysialylated neural cell adhesion molecule (NCAM-H) is expressed by newly generated granule cells in the dentate gyrus of the adult rat. J. Neurosci. **13:**2351–2358.
44. **Sferra, T. J., G. Qu, D. McNeely, R. Rennard, K. R. Clark, W. D. Lo, and P. R. Johnson.** 2000. Recombinant adeno-associated virus-mediated correction of lysosomal storage within the central nervous system of the adult mucopolysaccharidosis type VII mouse. Hum. Gene Ther. **11:**507–519.
45. **Shepherd, G. M.** 1974. The synaptic organization of the brain: an introduction. Oxford University Press, New York, N.Y.
46. **Skorupa, A. F., K. J. Fisher, J. M. Wilson, M. K. Parente, and J. H. Wolfe.** 1999. Sustained production of β-glucuronidase from localized sites after AAV vector gene transfer results in widespread distribution of enzyme and reversal of lysosomal storage lesions in a large volume of brain in mucopo-

lysaccharidosis VII mice. Exp. Neurol. **160:**17–27.
47. **Snyder, E. Y., R. M. Taylor, and J. H. Wolfe.** 1995. Neural progenitor cell engraftment corrects lysosomal storage throughout the MPS VII mouse brain. Nature **374:**367–370.
48. **Stein, C. S., A. Ghodsi, T. Derksen, and B. L. Davidson.** 1999. Systemic and central nervous system correction of lysosomal storage in mucopolysaccharidosis type VII mice. J. Virol. **73:**3424–3429.
49. **Summerford, C., and R. J. Samulski.** 1998. Membrane-associated heparin sulfate proteoglycan is a receptor for adeno-associated virus type 2 virions. J. Virol. **72:**1438–1445.
50. **Taylor, R. M., and J. H. Wolfe.** 1997. Decreased lysosomal storage in the adult MPS VII mouse brain in the vicinity of grafts of retroviral vector-corrected fibroblasts secreting high levels of beta-glucuronidase. Nat. Med. **3:**771–774.
51. **Walsh, C., and C. L. Cepko.** 1988. Clonally related cortical cells show several migration patterns. Science **241:**1342–1345.
52. **Walsh, C., and C. L. Cepko.** 1992. Widespread dispersion of neuronal clones across functional regions of the cerebral cortex. Science **255:**434–440.
53. **Wolfe, J. H., J. W. Kyle, M. S. Sand, W. S. Sly, D. G. Markowitz, and M. K. Parente.** 1995. High level expression and export of β-glucuronidase from murine mucopolysaccharidosis VII cells corrected by a double-copy retrovirus vector. Gene Ther. **2:**70–78.
54. **Wolfe, J. H., and M. S. Sands.** 1996. Murine mucopolysaccharidosis type VII: a model for somatic gene therapy of the central nervous system, p. 263–274. *In* R. R. Lowenstein and L. W. Enquist (ed.), Protocols for gene transfer in neuroscience: towards gene therapy of neurological disorders. John Wiley & Sons Ltd., London, United Kingdom.
55. **Wu, P., M. I. Phillips, J. Bui, and E. F. Terwilliger.** 1998. Adeno-associated virus vector-mediated integration into neurons and other nondividing cell targets. J. Virol. **72:**5919–5926.
56. **Xiao, X., J. Li, T. J. McCown, and R. J. Samulski.** 1997. Gene transfer by adeno-associated virus vectors into the central nervous system. Exp. Neurol. **144:**113–124.
57. **Yoon, S. O., C. Lois, M. Alvirez, A. Alvarez-Buylla, E. Falck-Pedersen, and M. V. Chao.** 1996. Adenovirus-mediated gene delivery into neuronal precursors of adult mouse brain. Proc. Natl. Acad. Sci. USA **93:**11974–11979.